

## CHARACTERIZATION OF ZnS/ ZnSe QUANTUM WELLS GROWN BY PHOTOASSISTED VAPOUR PHASE EPITAXY

M. P. HALSALL, V. V. TISHCHENKO<sup>1</sup>, A. V. KOVALENKO<sup>2</sup>, J. E. NICHOLLS<sup>3</sup>, P. LILLEY<sup>4</sup>

UDC 535.37:537.311.33

№ 2001

Department of Physics (UMIST Manchester M60 1QD, U.K.),

<sup>1</sup>Institute of Physics, Nat. Acad. Sci. of Ukraine (46, Nauky Ave., Kyiv 03028 Ukraine: vvti@iop.kiev.ua),

<sup>2</sup>Dnipropetrovsk University (72, Gagarina Ave., Dnipropetrovsk 49625, Ukraine),

<sup>3</sup>Department of Applied Physics, University of Hull (Hull HU6 7RX, U.K.),

<sup>4</sup>Department of Electrical Engineering, University of Manchester (Manchester M13 9PL, U.K.)

Research into light emitting applications for ZnSe/ZnS materials presently centers on the materials grown epitaxially by either MOVPE or MBE techniques. If a simpler technique could be found to reproduce the material quality obtained by MBE or MOVPE, this would be preferred. This paper reports the growth of good quality ZnS/ZnSe quantum well structures on GaAs at very low temperatures by the technique of photoassisted vapour phase epitaxy (PAVPE). The structures were assessed by low temperature photoluminescence and Raman spectroscopy. Both techniques show the effects of reduced dimensionality. A new lattice dynamic model appropriate for strained systems is used to derive the ZnSe strain state and well width for the samples studied.

For many years, the ZnS/ZnSe system has been the focus of much attention for applications in all solid-state blue and green light emitting devices, although traditionally these materials have always suffered from the lack of controlled *p*-type doping needed to produce light emitting *p-n* junctions. The most recent research has centered on the controlled production of *p*-type ZnSe/ZnS/ZnCdSe quantum well structures and ZnMgSSe materials by incorporation of atomic nitrogen during MBE growth [1, 2]. More recently, some success has been reported for the growth of *p*-type ZnSe/ZnS structures by MOVPE [3]. If these materials are going to be viable choices for use in mass produced blue and green light emitting devices, an alternative method of growth is preferable since both MBE and MOVPE are expensive techniques. Moreover, in the case of MOVPE, efficient *p*-doping agents have yet to be found and hydrogen incorporation from the sources is suspected of playing a role in passivation of doping species in ZnSe [4]. Here, we report an initial investigation of the possibility of optoelectronic material production by the comparatively simple technique of photoassisted vapour phase epitaxy (PAVPE) as well as the production of good quality ZnSe quantum wells in ZnS barriers by PAVPE.

Photoassisted techniques rely on the illumination of a growing layer with above band gap light to improve layer quality, as has been successfully demonstrated for ZnSe by MBE growth [5]. Here, we describe the application of the technique to the much simpler VPE

growth method. Some preliminary findings for ZnSe have already been reported [6]. With this technique, we have demonstrated the growth of high quality material at low growth at low temperatures using only high purity ZnSe and ZnS as source materials. For this study, a series of ZnS/ZnSe/ZnS quantum wells were prepared by PAVPE and assessed by low temperature photoluminescence and Raman spectroscopy.

A new method of calculating phonon frequencies in strained microstructures was used to analyze the Raman results and extract strain and layer thickness information.

The ZnS/ZnSe/ZnS on GaAs structures were grown in a horizontal, cylindrical quartz reactor with three axial channels for the vaporization of source materials. The vaporized materials were transported to the low temperature deposition regions by forced transport in a stream of high-purity hydrogen. The fourth input channel provides means for a further flow of hydrogen to provide vapour mixing and dilution of the reagents immediately before deposition on the GaAs substrate. The source materials were high-purity ZnS and ZnSe powders vaporized at 975 °C. Corrections to stoichiometry were made by the use of evaporation of elemental sources of Zn, S, and Se. The structures can be grown in the temperature range 170 - 350 °C. The apparatus provides for a large temperature gradient in the deposition zone. Photoassisted growth is achieved by illumination of the substrate during growth by approximately 0.8 W/cm<sup>2</sup> of light from a 442 nm He-Cd laser. The growth cycle is computer-controlled and has previously produced high quality ZnS and ZnSe single layers. The growth rate was 1.5 μm/h.

The photoluminescence measurements were taken with the samples immersed in liquid helium at 1.6 K and excited with the 351 nm line of an argon laser. The Raman spectra were taken at room temperature with the 514 nm line of the argon laser as a light source. The light was dispersed with a Spex 1404 spectrometer and detected with an intensified diode array detector. Fig. 1 shows the photoluminescence spectra taken from samples 366 and 381 with ZnSe

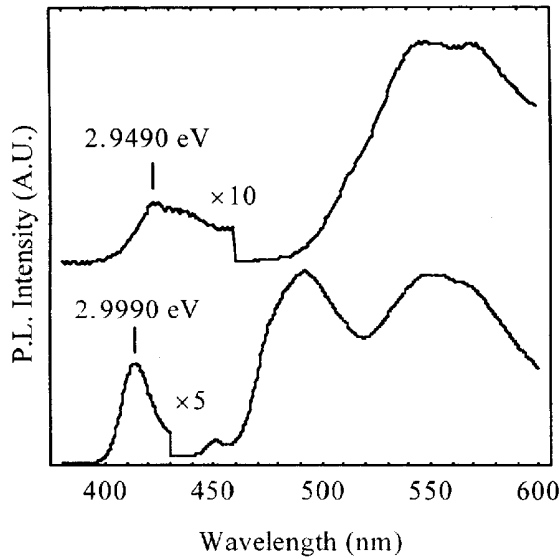


Fig. 1. Low temperature photoluminescence spectral regions of samples 366 (top) and 381, two ZnS/ZnSe/ZnS quantum wells with nominal well widths of 1.1 and 6.5 nm, respectively

well thicknesses estimated by growth rates of 1.1 and 6.5 nm, respectively. As can be seen, both samples show features, we ascribe to the recombination of excitons localized by well width fluctuations, at higher energy (their excitonic nature is confirmed by low temperature reflectivity measurements) as well as strong emission bands which may be due to impurities but are more likely to be due to misfit dislocations; enhanced deep emission has also been observed in thin layers of ZnSe [7] grown by other techniques and has been assigned to the onset of misfit dislocations in the thin layers. The spectra show the clear evidence of quantum confinement in that the excitonic emission is shifted to higher energy than that of bulk ZnSe. The transitions are marked in Fig. 1. We ascribe the higher energy luminescence peaks to excitons confined in the quantum wells, these occur at 2.9990 and 2.9400 eV for samples 381 and 366, respectively. These lines are shifted relative to the free ZnSe excitonic transition energy by 196.3 and 137.3 meV, respectively. To estimate the confinement effect, we use a simple effective mass calculation. We assume that, for such thin layers, the growth is pseudomorphic to GaAs (as is confirmed by the Raman measurements below). When strained biaxially along [100] and [010] axes, the heavy and light hole band gap of ZnSe can be expressed as [8].

$$E_{g,l,h}^{\text{ZnSe}} = 2.8207 + 1.67 \epsilon \quad E_{g,h,h}^{\text{ZnSe}} = 2.8207 + 4.45 \epsilon,$$

where the in-plane strain  $\epsilon = \epsilon_{xx} = \epsilon_{yy}$  (we define  $\epsilon$  to be positive for compressive stress). The lattice

mismatches between the GaAs substrate and ZnS and ZnSe are 0.27 and 4.4%, respectively. From this, we should expect a ZnSe band gap of 2.8255 eV when grown pseudomorphic to GaAs. We take conduction and valence band offsets of 68 and 824 meV, respectively [9]. We use carrier effective masses of  $m_e = 0.16 m_0$  and  $m_{h,h} = 1.45 m_0$  in both the well and barrier (the calculation is relatively insensitive to the ZnS effective masses), and we estimate the excitonic binding energy by the semiempirical approach described in [10]. Using a simple Kronig-Penney calculation with these parameters allows us to deduce the effective well widths of 1.3 and 1.8 nm for samples 381 and 366, respectively. These values can be compared to those found by the Raman measurements below. Although it is clear from the luminescence that the wells contain some intrinsic defects, given that the wells are pure ZnSe (as indicated by the Raman measurements below), the blue shift observed in the excitonic luminescence is the clear evidence for the confinement of carriers in the quantum wells. In order to deduce the degree of homogeneity of the wells, it would be necessary to compare photoluminescence with PLE and/or reflectivity measurements. In the absence of such a study, we simply observe that the full width half maxima of the excitonic peaks are of the order of 90 meV indicating that the well widths are defined to within  $\pm 1$  monolayer.

In addition to photoluminescence. Raman spectroscopy was used to study the quantum well composition and strain. The Raman spectra for samples 366, 367, 379, and 381 are shown in Fig. 2. The spectra were all taken in the back scattering geometry with polarization in the standard notation  $z[x'x']z$ , where the  $z$  direction is along the [100] axis and the  $x$  along the [011] axis. In this geometry, the longitudinal optical modes are allowed and the transverse modes forbidden. The spectra all show a strong GaAs LO signal and a weak GaAs TO mode (selection rules being slightly relaxed by the presence of some in-plane component of the light wave vector). In addition, two other signals are present to varying degrees located in the regions of 205 and 250  $\text{cm}^{-1}$ . We identify the two modes as being due to confined ZnSe TO and LO phonons, respectively. The wavelength of light used (514 nm) is close to the ZnSe band edge at room temperature and so the resonant enhancement of ZnSe modes is expected. For the same reason, the corresponding ZnS modes are not observed as the wavelength of light used is below the ZnS bandgap, and no resonant enhancement occurs. That the TO mode is observed is not surprising, as the relaxation of selection rules by interface disorder has been observed in other heterojunction systems. In thick ZnSe layers, the TO and LO modes have the measured frequencies of 205 and 254  $\text{cm}^{-1}$ , respectively (in the same geometry). Clearly in the case of our samples,

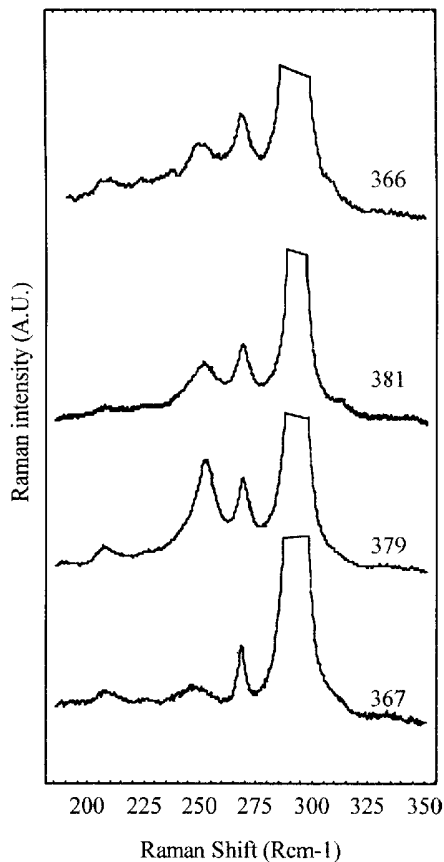


Fig. 2. Room temperature Raman spectra for four samples studied here. The spectra were taken in the  $z[x'x']z$  geometry with  $z$  and  $x'$  corresponding to the [001] and  $x' = [110]$  crystallographic axes, respectively. The strong signals at 269 and 293  $\text{cm}^{-1}$  are due to the GaAs TO and LO phonons, respectively. The peaks in the regions 250 and 205  $\text{cm}^{-1}$  are ascribed as due to the ZnSe LO and TO modes from the quantum well

there is a systematic shift to lower frequency in the LO mode with the decreasing well width. We ascribe this to confinement of the ZnSe LO mode in the quantum well and analyze the frequencies with a lattice dynamic model incorporating strain, the details of which will be reported elsewhere.

The phonon dispersion relations of ZnS and ZnSe were described by other workers [11, 12], in essence, the optical branch of the ZnSe phonon dispersion curves lies in the acoustic-optical phonon gap of ZnS, and so optical phonons are confined to the ZnSe layer in ZnSe/ZnS heterostructures and zone folding occurs. In addition, the 0.27% strain present in the phonon layer shifts the phonon frequencies via first-order changes in the nearest neighbour force constants. The ZnSe TO mode is nearly dispersionless for the wave

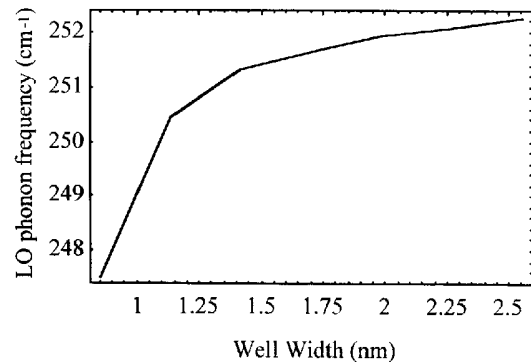


Fig. 3. ZnSe first confined LO phonon frequency for a ZnSe quantum well in ZnS barriers calculated as a function of well width. A strain of 0.27% is assumed as appropriate for pseudomorphic growth

vector along the [001] axis. Thus, the position of this mode is sensitive only to the strain present in the quantum well. The ZnSe LO mode is strongly dispersive and a measure of the two frequencies allows an estimation of both the strain state and quantum well thickness.

We assume that the observed phonon modes are due to the  $n = 1$  first confined TO and LO modes, as these are allowed in the scattering geometry used and, for quantum wells in general, are observed to have the largest scattering cross-sections [13]. In addition, the thinnest well, sample 367, shows an additional peak at 225  $\text{cm}^{-1}$  which we believe is due to an interface mode and which is weakly visible in spectra from some of the other samples. This will be discussed in detail in a future publication. We calculate the details of the phonon spectra by the rigid ion model in which strain is incorporated directly via appropriately symmetrized corrections to the nearest neighbour force constants. The exact details of the calculation will be presented elsewhere but it is an extension of the rigid ion model as used by other workers for similar systems [14, 15]. The calculated LO phonon frequencies as a function of well width are plotted in Fig. 3. To measure the sample well thicknesses, we fit the observed Raman spectra using the appropriate Lorentzian line shapes (three Lorentzians in the case of sample 367). This allows a resolution of approximately 0.5  $\text{cm}^{-1}$  to be achieved. Fig. 4 shows fits to the data for samples 366 and 367.

It was found in all cases that the observed frequencies were consistent with a 0.27% compressive strain as expected for pseudomorphic growth. The well widths indicated by Raman and PL along with nominal values are listed in Table. For the wider wells, the Raman measurements are more unreliable due to the reduced effect of mode confinement, but it is clear that the nominal widths were not achieved during the growth for two wider samples. In addition, there is

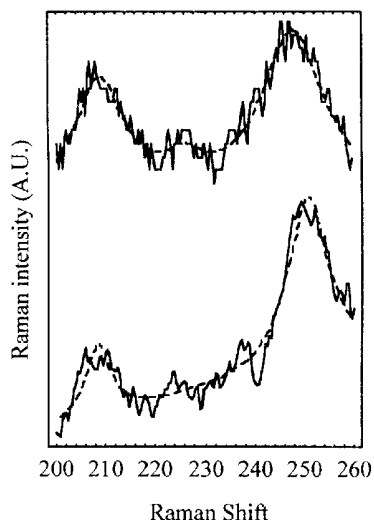


Fig. 4. Fitting of the ZnSe phonon spectral region for samples 366 and 367. Lorentzians are summed to form a simulation of the observed spectrum and allow the accurate measurement of phonon frequencies. Sample 366 has an additional peak at 225 cm<sup>-1</sup> as discussed in the text

a discrepancy between the thicknesses measured in the case of sample 381. We believe this is due to interface disorder, to which the two techniques have different sensitivities (the discrepancy corresponds to a variation in the well width of 4 monolayers). Clearly, the photoluminescence measurements can only give a very approximate estimate of the well band gap. In

Nominal and characterized parameters of the samples described

Sample	$\omega_{LO}$ (cm <sup>-1</sup> )	$\omega_{TO}$ (cm <sup>-1</sup> )	$L_w^{nominal}$ (nm)	$L_w^{Raman}$ (nm)	$L_w^{PL}$ (nm)
367	247.8	208.7	1.1	0.85	-
379	252.2	207.4	6.5	≈ 2.8	-
381	252.2	207.8	6.5	≈ 2.8	1.3
366	250.7	208.5	1.1	1.1	1.7

the absence of photoluminescence excitation measurements, the presence of any Stokes shift is unknown, and well width variations are a possible source of the discrepancy in the measured thicknesses for this sample. In general, Raman measurements provide a more reliable guide to the physical structure of samples, and the Raman spectra presented here clearly show the presence of well-defined ZnSe wells in ZnS barriers and indicate a good degree of structural uniformity. In conclusion, we have described a simple and efficient alternative photo-assisted technique for the growth of II-VI microstructures. The design of a VPE reactor enables the growth of II-VI materials at low growth temperatures and rates. The materials were characterized by low temperature photoluminescence and room temperature Raman scattering techniques. Together the characterization techniques indicate the growth of good quality ZnS/ZnSe quantum wells.

- Haase M.A., Qiu J., DePuydt J.M., Cheng H.//Appl. Phys. Lett. 1991. **59**, N11. P.1272 - 1274.
- Iton S., Nakayama N., Ohata T. et al.//Jap. J. Appl. Phys. 1994. **33**, N5a. P.L639 - L642.
- Miyachi M., Ohira Y., Komatsu S. et al.//J. Cryst. Growth. 1996. **159**. P.261 - 266.
- Yasuda T., Yasui T., Zhang B., Segawa Y.//Ibid. P.1168 - 1172.
- Matsumura N., Fukada T., Sakamoto T.//Ibid. 1990. **101**. P.61 - 64.
- Kovalenko A.V. and Tishchenko V.//Jap. J. Appl. Phys. 1995. **34**. P.209 - 211.
- Shibata N., Ohki A., Zembutsu S., Katsui A.//Ibid. 1988. **27**, N3. P.L441 - L443.
- Potts J.E., Cheng H., Mohapatra S., Smith T.L.//J. Appl. Phys. 1987. **61**, N1. P.333 - 339.
- Yamada Y., Masumoto Y., Taguchi T.//Surf. Sci. 1992. **267**, N1. P.129 - 133.
- Mathieu H., Lefebvre P., Christol P.//J. Appl. Phys. 1992. **72**, N1. P.300 - 312.
- Vagelatos N., Wehe D., King J.S.//J. Chem. Phys. 1974. **60**, N9. P.3613 - 3618.
- Henion B., Moussa F., Pery G. and Kunc K.//Phys. Letts. 1971. **36A**, N5. P.376 - 378.
- Cui J., Wang H. and Gan F.//J. Appl. Phys. 1992. **72**, N4. P.1521 - 1527.
- Vetelino J.F. and Mitra S.S.//Solid State Commun. 1969. **7**, N17. P.1181 - 1186.
- Ren S., Chu H. and Chang Y.//Phys. Rev. B. 1988. **37**, N5. P.8899 - 8911.

Received 25.12.00